On the role played by the chalcogen donor atoms in diimine-dichalcogenolate Pt^{II} SONLO chromophores: is it worth replacing sulfur with selenium?

Anna Pintus,[‡] M. Carla Aragoni,[‡] Francesco Isaia,[‡] Vito Lippolis,[‡] Dominique Lorcy,[†] Alexandra M. Z. Slawin,[§] J. Derek Woollins,[§] and Massimiliano Arca*[,‡] [†§]

[‡] Dipartimento di Scienze Chimiche e Geologiche, Università degli Studi di Cagliari, S.S. 554 bivio per Sestu, 09042 Monserrato (CA), Italy

[†] Sciences Chimiques de Rennes, UMR 6226 CNRS-Université de Rennes 1, Campus de Beaulieu, 35042 Rennes Cedex, France

[§] EaStCHEM School of Chemistry, University of St. Andrews, North Haugh, St. Andrews, Fife, KY16 9ST, UK

Supporting Information Placeholder

ABSTRACT: Two new diimine-diselenolate Pt^{II} chromophores [Pt(bipy)(Me-dset)] (**1**) and [Pt(phen)(Me-dset)] (**2**) (Me-dset^{2-} = *N*-methyl-2-thioxo-thiazoline-4,5-diselenolate) were synthesized and characterized. The effect of replacing sulfur with selenium was investigated by comparing the UV/Vis spectroscopic and electrochemical properties of **1** and **2** with those of the corresponding sulfur analogues, [Pt(bipy)(Me-dmet)] (**4**) and [Pt(phen)(Me-dmet)] (**5**), with a particular focus on their linear and nonlinear optical properties.

Since the advent of the laser, the search for nonlinear optical (NLO) chromophores has received considerable attention.[1,2] Among the coordination compounds suitable as NLO materials,[3,4,5] dimmine-dithiolate platinum(II) complexes [Pt(N^N)(S^S)] [6,7,8] have been exploited in applications as varied as dye-sensitized solar cells,[9,10,11] light-to-chemical energy conversion,[12,13] and DNA intercalation.[14,15] In the search for structure-property relationships within this class of compounds, the effect of the substituents on both the diimine and the dithiolate ligands has been systematically investigated.[16,17,18,19] In this context, we recently synthesized a series of platinum diimine-dithiolate systems bearing S^S ligands belonging to the class R-dmet^{2-} (*N*-alkyl and aryl-substituted 2-thioxo-thiazoline-4,5-dithiolate),[20,21] which showed promising second order NLO (SONLO) properties.[22]

Surprisingly, little attention has been paid toward the variation in the coordinating atoms of these compounds, and to date only a single example of a diimine-diselenolate Pt^{II} complex has been reported, namely [Pt(bipy)(bds)] (bipy = 2,2'-bipyridine, bds^{2-} = benzene-1,2-diselenolate).[23]

Scheme 1. Molecular scheme of complexes 1 and 2.

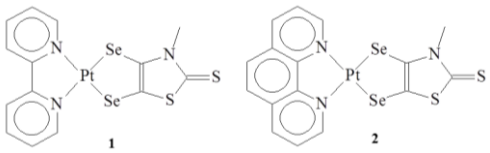

Starting from the common precursor *N*-methyl-4,5-*bis*-(2'-cyanoethylseleno)1-3-thioazol-2-thione, two novel diimine-diselenolate complexes, [Pt(bipy)(Me-dset)] (**1**) and [Pt(phen)(Me-dset)] (**2**, phen = 1,10-phenanthroline; Scheme 1), were synthesized (Scheme S1 in Supporting Information, SI).[24,25] The single-crystal X-ray analysis of **1**·1/2CH_2Cl_2 (Fig. 1; Fig. S1, Tables S1–S5 in SI)[26] shows the complex is almost completely planar but for the methyl substituent at the diselenolate,[27] the metal ion featuring a square planar coordination by the two chelate ligands.[28] Both the Pt–Se and, to a minor extent, the Pt–N distances [2.3803(13)–2.3929(21) and 2.078(9)–2.060(9) Å, respectively] are longer than the corresponding mean bond lengths observed for [Pt(N^N)(S^S)] systems.[29] A direct comparison of the Pt–E distances in **1** (E = Se) and the closely relat-

ed sulfur analogue [Pt(bipy)(Et-dmet)] (**3**; E = S)[22] shows that the lengthening (0.12 Å) is slightly smaller than the covalent radius difference between the two chalcogen atoms (0.15 Å).[30]

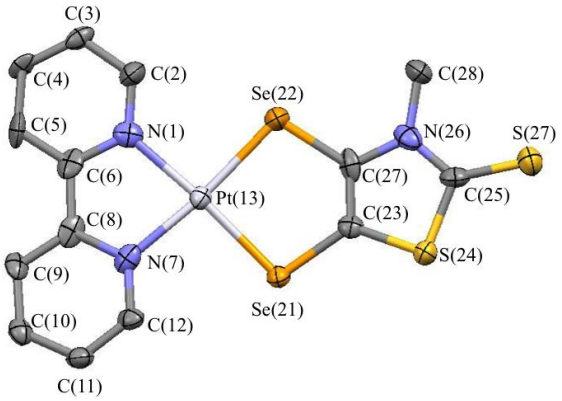

Figure 1. ORTEP drawing of complex **1** in **1**·1/2CH_2Cl_2 showing the atom-labeling scheme. Thermal ellipsoids are drawn at the 60% probability level. H atoms have been omitted for clarity.

The crystal packing of **1**·1/2CH_2Cl_2 (Fig. S1 in SI) mainly arises from two main different types of interactions, both contributing to form stacks developing along the *a* direction: (i) slipped π–π stacking interactions between the 2,2'-bipyridine rings of symmetry related molecules in head-to-head orientation (intercentroid distance 3.60 Å), and (ii) face-to-face interactions between the 2,2'-bipyridine and the C_3NS heterocycle of the Me-dset^{2-} ligand (intercentroid distance 3.50 Å).

Table 1. Absorption maxima λ_{max} (nm) and molar extinction coefficients ε (M^{-1} cm^{-1}) for the Vis absorption, half-wave potentials (V *vs* Fc^+/Fc),[a] emission maxima λ_{em}, and quantum yields Φ[b] for 1, 2, 4 and 5 in dmso solution at 298 K.

	1	**2**	**4**[c]	**5**[c]
λ_{max}	569	570	581	581
ε	3500	5000	4300	5000
$E_{1/2}^{I}$	0.044	−0.027	−0.004	−0.017
$E_{1/2}^{II}$	−1.607	−1.620	−1.608	−1.620
$E_{1/2}^{III}$	−2.245	/	−2.270	/
λ_{em}	374, 394	373, 392	374, 395	372, 405
Φ	$8.2\cdot10^{-3}$	$1.8\cdot10^{-2}$	$1.2\cdot10^{-2}$	$8.2\cdot10^{-3}$

[a] Supporting electrolyte 0.10 M $TBAPF_6$, Ag/AgCl reference electrode, scan rate 50 mV s^{-1}. [b] Quantum yields determined by using anthracene in ethyl alcohol solution as reference. [c] Taken from Ref. 22.

Cyclic voltammetry measurements performed in dmso on **1** and **2** (Table 1; Table S6 and Fig. S2 in SI for **1**) showed the presence of a *quasi* reversible oxidation process (i_{pc}/i_{pa} = 0.5–0.9) falling at $E_{1/2}^{I} \approx$ 0.0 V *vs* Fc^+/Fc for both complexes, and a reversible reduction (i_{pc}/i_{pa} = 1.1–1.2) with $E_{1/2}^{II}$ at about −1.6 V *vs* Fc^+/Fc. The two redox processes correspond to the conversion of the neutral complexes into their monocationic and monoanionic species, respectively.[31] Complex **1** features a further reversible monoelectronic reduction (i_{pc}/i_{pa} = 0.8; $|E_{pc} - E_{pa}|$ = 0.048 V) at $E_{1/2}^{III}$ = −2.245 V *vs* Fc^+/Fc. Given the shift toward more negative values observed for the $E_{1/2}^{II}$ reduction upon passing from complex **1** to complex **2**, 1,10-phenanthroline in place of 2,2'-bipyridine possibly causes a slight destabilization of the LUMO, preventing the $E_{1/2}^{III}$ reduction to be observed for complex **2** within the explored potential range. No significant changes can be observed in the potentials of the $E_{1/2}^{II}$ reduction of **1** and **2** as compared to those of the sulfur analogues [Pt(N^N)(Me-dmet)] [N^N = bipy (**4**) and phen (**5**)].[22] On the other hand, the $E_{1/2}^{I}$ oxidation potential is slightly shifted towards more positive potentials in the case of the selenated systems.

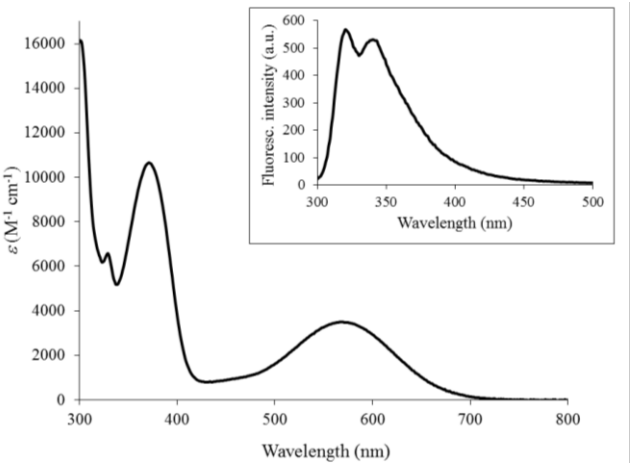

Figure 2. Absorption and emission (inset; λ_{exc} = 341 nm) UV/Vis spectra recorded for **1** in dmso.

UV/Vis/NIR absorption spectra recorded for **1** and **2** in dmso show a broad band with absorption maxima λ_{max} at about 570 nm (Table 2 and Fig. 2 for **1**). Absorption spectra recorded in eight different solvents (namely CH_2Cl_2, $CHCl_3$, CH_3CN, acetone, thf, dmf, dmso, and toluene), show a remarkable negative solvatochromic behavior ($\Delta\lambda_{max} \approx$ 150 nm for **1**) of the Vis band. A linear correlation was found between the experimentally measured λ_{max} visible absorption maxima recorded for **1** and **2** and the empirical parameters reported by Eisenberg and coworkers for diimine-dithiolate Pt^{II} systems (Fig. S3 in SI for

1).[6] A blue shift of this absorption band was found for **1** and **2** as compared to **4** and **5**.[22] Fluorescence spectroscopy measurements performed on solutions of **1** and **2** in dmso at room temperature (C = $3{\cdot}10^{-7}$–$3{\cdot}10^{-5}$ M; Fig. 2 for **1**), showed an emission with maxima λ_{em} at about 370 and 390 nm, whose intensity tends to decrease upon increasing the concentration of the solution, possibly due to self-quenching processes.[32] The analogy with the emission properties of **4** and **5** suggests a similar origin for the fluorescent emission of all of the complexes, which therefore should not involve the E^E ligand.[22]

Table 2. Absorption maxima λ_{max} (nm) and molar extinction coefficients ε (M^{-1} cm^{-1}) of the Vis absorption of 1 and 2 in different solvents.

	1		**2**	
	λ_{max}	ε^a	λ_{max}	ε^a
CH_2Cl_2	622	5100	618	4300
$CHCl_3$	647	5400	644	3600
CH_3CN	578	3200	570	3400
acetone	590	3500	601	/
thf	635	4200	637	2800
dmf	575	4600	577	5200
dmso	569	3500	570	5000
toluene[b]	732	/	/	/

[a] If not reported, the molar extinction coefficients were not determined for solubility reasons. [b] The spectrum of **2** in toluene could not be registered due to solubility reasons.

The structure of **1** optimized at density functional theory (DFT)[33] level (Table S7 in SI) shows a very good agreement with the corresponding structural data (the principal bond distances and angles being varied by less than 0.01 Å and 2°, respectively).[34] As found experimentally, a strengthening of the Pt–E bonds and a concurrent lengthening of the Pt–N distances was computed on passing from sulfured to selenated complexes.[35] Accordingly, the calculated values of Wiberg bond indices (WBIs)[36] for Pt–E and Pt–N bonds are larger and smaller, respectively, for **1** and **2** as compared to **4** and **5**,[37] and the second-order perturbation analysis of the Fock matrix in the NBO basis[38] showed that in the selenated systems the the interaction between the N lone pairs and the Pt unfilled natural orbitals is weaker than in the corresponding sulfur complexes.[39] The frontier Kohn-Sham (KS) MO scheme calculated for **1** (Fig. 3) shows the KS-HOMO is centered on the Me-dset^{2-} ligand and the KS-LUMO on the diimine (91 and 93%, respectively, in CH_2Cl_2; Table S8 and Fig. S4 in SI for **1**). In agreement with electrochemical data, a slight stabilization of the KS-LUMO was calculated on passing from **1** to **2** (E = –2.69 and –2.65 eV, respectively, in CH_2Cl_2). A stabilization of the KS-HOMO of **1** and **2** as compared to **4** and **5** was also computed (E = –4.87 eV for both complexes in CH_2Cl_2), thus accounting for the shift of the oxidation potentials observed experimentally. A natural population analysis (NPA)[38] shows that the Me-dset^{2-} ligand carries a negative charge of about –0.6e in CH_2Cl_2 (Table S9 in SI), whilst the diimine bears a partial positive charge of about 0.5e, the remaining positive charge (0.1e) being carried by the metal. This results in a net charge separation of about 1.1e for both **1** and **2**.

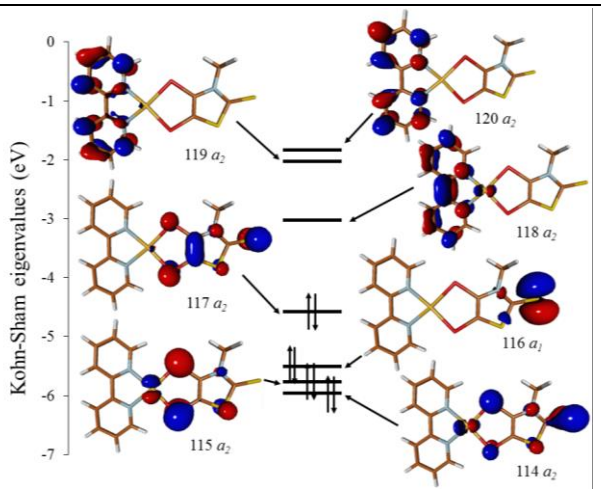

Figure 3. KS-MO scheme and isosurface drawings calculated for **1** in the gas phase (C_s point group; contour value = 0.05 e).

Time-dependent (TD) DFT calculations carried out on complexes **1** and **2** in their ground states in the same solvents used for UV/Vis/NIR measurements provided simulated spectra in very good agreement with the experimental ones (Fig. S10 in SI for **1**). The solvatochromic band is assigned to the $S_0 \rightarrow S_1$ vertical transition, which in turn derives (99% for **1**) from the KS-HOMO→KS-LUMO monoelectronic excitation (Table S10 in SI for **1**). This interligand charge-transfer (ILCT) process from the Me-dset^{2-} ligand to the diimine accounts for the negative solvatochromism of the corresponding absorption, and for the blue shift observed on passing from [Pt(N^N)(Me-dmet)] to [Pt(N^N)(Me-dset)] complexes.[22]

Finally, the values of static dipole moments (μ) and first static hyperpolarizabilities (β_{tot}) were calculated (Table S11 in SI), showing no significant differences

between [Pt(N^N)(Me-dset)] and [Pt(N^N)(R-dmet)] systems, thus indicating that the value of β_{tot} is mostly influenced by the diimine.[22]

In summary, the role played by the chalcogen donor atom on the properties of platinum diimine-dichalcogenolate complexes [Pt(N^N)(Me-dmet/Me-dset)] was elucidated, showing that selenium replacing sulfur induces a strengthening in the Pt–E bonds and a weakening of the Pt–N ones, resulting in a stabilization of the HOMO. This in turn causes a shift in the oxidation potentials toward more positive values, and a blue shift of the characteristic solvatochromic absorption band in the visible region. The hyperpolarizability (β_{tot}) calculations performed on the title complexes indicate diimine-dichalcogenolate Pt^{II} complexes as promising candidates for applications such as second harmonic generation (SHG), although the replacement of sulfur with selenium does not influence their β_{tot} and thus the possibility for SONLO applications.

ASSOCIATED CONTENT

Supporting Information. Detailed information about the synthesis and characterization of complexes **1** and **2**, crystallographic data and packing details for **1**·1/2CH_2Cl_2, electrochemical, solvatochromic and fluorescence features of the title compounds, computational setup employed for the DFT calculations, metric parameters, frontier molecular orbitals eigenvalues and composition, natural atomic charges, singlet electronic transitions and simulated spectra, static first hyperpolarizability and dipole moment values calculated in the gas phase and/or in CH_2Cl_2. This material is available free of charge via the Internet at http://pubs.acs.org.

AUTHOR INFORMATION

Corresponding Author

*E-mail: marca@unica.it.

Author Contributions

The manuscript was written through contributions of all authors. All authors have given approval to the final version of the manuscript.

Funding Sources

No competing financial interests have been declared.

ACKNOWLEDGMENT

The Università degli Studi di Cagliari, the Ministero dell'Istruzione, dell'Università e della Ricerca (MIUR, PRIN 2009Z9ASCA) and the Regione Autonoma della Sardegna are acknowledged for financial support. M. Arca thanks the Consorzio interuniversitario per le Applicazioni di Supercalcolo Per Università e Ricerca (CASPUR) for providing computational resources within the framework of HPC grants 2012.

REFERENCES

1 Christodoulides, D. N.; Khoo, I. C.; Salamo, G. J.; Stegeman, G. I.; Van Stryland, E. W. *Adv. Opt. Photon.* **2010**, *2*, 60–200.

2 *Non-Linear Optical Properties of Matter: From Molecules to Condensed Phases*, Papadopoulos, M. G.; Sadlej, A. J.; Leszczynski, J., Eds.; Springer: Dordrecht, The Netherlands, 2006.

3 Di Bella, S. *Chem. Soc. Rev.* **2001**, *30*, 355–366.

4 Zhang, C.; Song, Y.; Wang, X. *Coord. Chem. Rev*. **2007**, *251,* 111–141.

5 Humphrey, M. G.; Cifuentes, M. P.; Samoc, M. *Top. Organomet. Chem*. **2010**, *28*, 57–73.

6 Cummings S. D.; Eisenberg, R. *J. Am. Chem. Soc.* **1996**, *118,* 1949–1960.

7 Mitsopoulou, C. A. *Coord. Chem. Rev.* **2010**, *254*, 1448–1456.

8 Chen, C.-T.; Liao, S.-Y.; Lin, K.-J.; Chen, C.-H.; Lin, T.-Y. J. *Inorg. Chem.* **1999**, *38,* 2734–2741

9 Geary, E. A. M.; Yellowlees, L. J.; Jack, L. A.; Oswald, I. D. H.; Parsons, S,; Hirata, N.; Durrant, J. R.; Robertson, N. *Inorg. Chem.* **2005**, *44*, 242–250.

10 Islam, A.; Sugihara, H.; Hara, K.; Singh, L. P.; Katoh, R.; Yanagida, M.; Takahashi, Y.; Murata, S.; Arakawa, H. *Inorg. Chem.* **2001**, *40*, 5371–5380.

11 Linfoot, C. L.; Richardson, P.; McCall, K. L.; Durrant, J. R.; Morandeira, A.; Robertson, N. *Solar Energy* **2011**, *85*, 1195–1203.

12 Hissler, M.; McGarrah, J. E.; Connick, W. B.; Geiger, D. K.; Cummings, S. D.; Eisenberg, R. *Coord. Chem. Rev.* **2000**, *208*, 115–137.

13 Zhang, J.; Du, P.; Schneider, J.; Jarosz, P.; Eisenberg, R. *J. Am. Chem. Soc.* **2007**, *129*, 7726–7727.

14 Mitsopoulou, C. A.; Dagas, C. E.; Makedonas, C. *Inorg. Chim. Acta* **2008**, *361,* 1973–1982.

15 Mitsopoulou, C. A.; Dagas, C. E.; Makedonas, C. *J. Inorg. Biochem.* **2008**, *102,* 77–86.

16 Geary, E. A. M.; McCall, K. L.; Turner, A.; Murray, P. R.; McInnes, E. J. L.; Jack, L. A.; Yellowlees, L. J.; Robertson, N. *Dalton Trans.* **2008**, 3701–3708.

17 Cummings, S. D.; Cheng, L.-T.; Eisemberg, R. *Chem. Mater.* **1997**, *9*, 440–450.

18 Paw, W.; Cumming, S. D.; Mansour, M. A.; Connick, W. B.; Geiger, D. K.; Eisenberg, R. *Coord. Chem. Rev.* **1998**, *171*, 125–150.

19 Pintus, A.; Aragoni, M. C.; Coles, S. J.; Coles, S. L.; Isaia, F.; Lippolis, V.; Musteti, A.-D.; Teixidor, F.; Vinas, C.; Arca, M. *Dalton Trans.* **2014**, *43*, 13649–13660.

20 Aragoni, M. C.; Arca, M.; Devillanova, F. A.; Isaia, F.; Lippolis, V.; Mancini, A.; Pala, L.; Slawin, A. M. Z.; Woollins, J. D. *Inorg. Chem.* **2005**, *44*, 9610–9612.

21 Eid, S.; Guerro, M.; Lorcy, D. *Tetrahedron Lett*. **2006**, *47*, 8333–8336.

22 Pintus, A.; Aragoni, M. C.; Bellec, N.; Devillanova, F. A.; Lorcy, D.; Isaia, F.; Lippolis, V.; Randall, R. A. M.; Roisnel, T.; Slawin, A. M. Z.; Woollins, J. D.; Arca, M. *Eur. J. Inorg. Chem.* **2012**, 3577–3594.

23 Dibrov S. M.; Bachman, R. E. *Inorg. Chim. Acta* **2004**, *357*, 1198–1204.

24 Also reported as Me-thiazds^{2-} in Ref. 25.

25 Eid S.; Formigué, M.; Roisnel, T.; Lorcy, D. *Inorg. Chem.* **2007**, *46*, 10647–10654.

26 The quality of the corresponding structure was unfortunately not excellent, as testified by its *R* index (see Table S1 in SI), probably due to the encapsulated solvent molecules.

27 N(7)–Pt(13)–Se(21)–C(23) dihedral angle = –169.6(4)°.

28 The crystal packing of **1**·1/2CH_2Cl_2 (Fig. S1) mainly arises from stacking interactions involving the 2,2'-bipyridine rings and the C_3NS heterocyclic moieties of the Me-dset^{2-} ligand, which lead to the formation of cavities occupied by disordered CH_2Cl_2 molecules.

29 An examination of the CDS (v. 5.33, updated Feb. 2014) provided to date 37 authentic examples of monomeric [Pt(N^N)(S^S)] complexes, showing average Pt–S and Pt–N bond lengths of 2.239(16) and 2.045(16) Å, respectively.

30 Cordero, B.; Gómez, V.; Platero-Prats, A. E.; Revés, M.; Echeverría, J.; Cremades, E.; Barragán, F.; Alvarez, *S. Dalton Trans.* **2008**, *21*, 2832–2838.

31 $|E_{pc} - E_{pa}|$ in the range 0.049–0.056 V; see Table S3 in SI.

32 Fleeman W. L.; Connick, W. B. *Comments Inorg. Chem.* **2002**, *23*, 205–230.

33 *A Chemist's Guide to Density Functional Theory*, Koch W.; Holthausen, M. C., 2nd ed.; Wiley-VCH: Weinheim, Germany, 2002.

34 No significant changes in the optimized structural parameters were observed upon considering implicit solvation in the calculations, all of the bond lengths and angles differing by less than 0.02 Å and 1°, respectively.

35 Average calculated Pt–S/Pt–N bond lengths in CH_2Cl_2= 2.277/2.056 and 2.274/2.064 Å for **4** and **5**, respectively.

36 Wiberg, K. *Tetrahedron* **1968**, 24, 1083–1096.

37 Average calculated Wiberg indices for Pt–E/Pt–N bonds = 0.797/0.476 (**1**), 0.800/0.469 (**2**), 0.7874/0.499 (**4**), and 0.798/0.499 (**5**) in CH_2Cl_2.

38 Reed, A. E.; Weinstock, R. B.; Weinhold, F. *J. Chem. Phys.* **1985**, *83*, 735–746.

39 Average calculated energies for the interactions between the lone pairs localized on the nitrogen atoms of the N^N ligand and the empty atomic orbitals on the Pt ion: 96.3 (**1**), 93.8 (**2**), 103.2 (**4**), 99.7 (**5**) kcal mol^{-1} in CH_2Cl_2.